Innovative Grid-Connected Photovoltaic Systems Control Based on Complex-Vector-Filter

Mansouri, Nouha; Nasri, Sihem; Lashab, Abderezak; Guerrero, Josep M.; Cherif, Adnen

Published in:
Energies

DOI (link to publication from Publisher):
10.3390/en15186772

Publication date:
2022

Document Version
Publisher's PDF, also known as Version of record

energies

MDPI

Article

Innovative Grid-Connected Photovoltaic Systems Control Based on Complex-Vector-Filter

Nouha Mansouri [1,2], Sihem Nasri [2], Abderezak Lashab [3], Josep M. Guerrero [3,*] and Adnen Cherif [2]

[1] Department of Electrical Engineering, National School of Engineering Monastir, Monastir 5035, Tunisia
[2] Department of Electronic Systems, Analysis and Treatment of Electrical/Energetic Systems Research Unit, Faculty of Sciences, Tunis 2092, Tunisia
[3] Department of Energy Technology, Center for Research on Microgrids (CROM), Aalborg University, Pontoppidanstraede 111, DK-9220 Aalborg, Denmark
* Correspondence: joz@energy.aau.dk

Abstract: The research presented in this paper explains how the complex-vector-filter (CVF) method can help in minimizing the current harmonic of a grid-tied photovoltaic system. In fact, the harmonic-free positive sequence (HFPS) load current is used to produce referential sinusoidal currents. This control stabilizes the grid's currents under unbalanced load currents, as well as mitigates undesirable harmonic load currents, while feeding clean active power to the grid. Thanks to the proposed controller, the performance, such as robustness, as well as the stability and dynamics of the CVF are more effective compared to the proportional-integral (PI) with phase-locked-loop (PLL) controller. Moreover, the CVF ensures robustness and stability during the synchronization between the photovoltaic (PV) generator and the utility grid system. The PI&PLL control presents higher active and reactive power fluctuations during synchronization. On the other hand, the CVF ensures the elimination of the reactive power fluctuations during synchronization. The performance of the proposed CVF is validated by simulation through MATLAB software. Under all conditions, the grid current, considering harmonics, is within the limits set by the IEEE-519 power quality standard, where a total harmonic distortion (THD) of 1.56% was achieved in the case of feeding a non-linear load.

Keywords: photovoltaic (PV); voltage stability; grid-connected; complex-vector-filter; harmonic current

Citation: Mansouri, N.; Nasri, S.; Lashab, A.; Guerrero, J.M.; Cherif, A. Innovative Grid-Connected Photovoltaic Systems Control Based on Complex-Vector-Filter. *Energies* **2022**, *15*, 6772. https://doi.org/10.3390/en15186772

Academic Editor: Alon Kuperman

Received: 14 January 2022
Accepted: 5 September 2022
Published: 16 September 2022

1. Introduction

As the population is increasing, the demand for electricity is continuously increasing, while fossil fuels are insufficient to fulfill the demands. Moreover, fossil fuels have a negative impact on the environment due to the emission of harmful gases during use. Therefore, the alternative solution for the demand is renewable energy sources (RES) [1].

RES are the major topic to be focused on, and with the awareness among the people, the demand in RES is tremendously increasing. Different RES exist in nature. From these various sources, the photovoltaic (PV) system is environmentally friendly and a significantly encouraging source. The PV energy experienced a very significant escalation in the last decades, due to cost production reductions which can facilitate fossil energy dispensing and allow for the transition toward the use of green energy sources [2,3].

However, with the increasing penetration level of PV in the grid, important fluctuations introduce serious power quality concerns [4]. On the power grid side, fluctuations, variation of frequency, variation of voltage, harmonic, etc., are some of the issues that should be dealt with in these systems [5]. Consequently, it becomes mandatory for PV systems to act in conformity with the technical and regulatory frameworks to ensure safe operation and reliable and efficient system set.

Power electronics and digital control technology play a vital role in the grid-connected PV systems, improving their operation and power quality at the point of common coupling

(PCC). In [6], different inverter topologies are used for PV systems connected to the grid. For example, the best classic topology is the voltage source converter (VSC), which can be used for small, medium, or large-scale grid connection. The same topology can be adopted for low-voltage or medium-voltage grid connection.

Grid-connected PV systems appear in the form of pulse width modulation (PWM) VSC, which can inject controlled active power (AP) and reactive power (RP) as needed. The output current of this converter needs to be filtered to prevent current harmonics near the switching frequency (SF) from being injected into the grid [7].

The L-type filter is known by simplicity and robustness for integration, analysis, and operation. However, currently, researchers increasingly focus on the LCL filter, which draws attention to the small size, weight, and cost needs of PV system grid interfaces [8]. Moreover, the LCL filter is the most adopted since it offers better attenuation of the switching harmonics compared to the simple L filter. This mainly lies in the fact that the LCL filter is of third order, which promotes the SF attenuation more effectively [8]. However, the existing filter-based damping is not preferred due to the limited frequency characteristics. In fact, LCL filters have resonance problems that cause oscillations and lead to instability issues. An efficient active damping strategy is proposed by adopting a PID control structure with two degrees of freedom (DOF). Using this controller, oscillations are damped by about 98% [9].

In [10], various methods are reviewed, and the control strategy of the converter based on grid-connected PV systems is shown. Indeed, some hysteresis, sinusoidal pulse width modulation (SPWM), space-vector pulse width modulation (SVPWM) based on proportional integral (PI), proportional resonance (PR), and linear quadratic regulator strategies are discussed in detail. Among them, the hysteretic current control (HCC) is considered robust and can provide a fast dynamic response. However, SF changes may put a burden on the controller design. In [11], a three-level hysteresis current control (HCC) method for grid-connected VSC was proposed. This method can connect PV panels to the grid and ameliorate the power quality of the PCC at the same time, in line with IEEE 1547.1 and IEEE 519 standards. The traditional HCC suffers from variation in SF, which leads to switching losses in the VSC, whereas the three-level HCC solves the problem of the switching frequency variation using the offset hysteresis band, thus it improves the control performance.

Voltage fluctuations, harmonics, unbalance, and distortion can be present in the grid. Using the VSC-based distribution static compensator (DSTATCOM) system can alleviate these types of power quality issues [12].

In the literature, the power quality issues related to the non-linear load are discussed. In [8], the use of LCL filters ensures the elimination of the distortions of the currents injected into the network, knowing that the technique of proportional-integral derivative control is integrated to guarantee the complete suppression of the resonance oscillations of the LCL filter. In [13], a fuzzy logic controller associated with a three-phase PV inverter is adopted, which ensures the PCC voltage regulation, as well as the mitigation of the distortions of the service current and the injection of the excess power in the grid. In this case, the presence of an unbalanced load leads to the appearance of unbalanced grid currents and subsequently participates in the injection of zero and negative sequence currents into the grid. The control techniques that are discussed in the literature are based on the mitigation of the harmonics of the current supplied to the distribution grid, which leads to the minimization of the reactive power load on the grid, to the feeding of the excess power to the distribution grid, and to the increase in the usefulness of the VSC. The PLL based on the synchronous reference frame is adopted to make the connection between the PV converter and the distribution grid and to compensate for the harmonic current of the load current [14]. However, the presence of an unbalanced load and noisy movement in the voltages of the electrical network lead to the appearance of a double frequency oscillation. Therefore, on the other hand, the integration of a low-pass filter is necessary, as it results in an unreliable dynamic behavior. To avoid this problem, a notch filter is integrated in [15] to eliminate the

phenomenon of double frequency oscillations. The drawback of using the notch filter is delicacy in the case of variation of the system parameters, which makes it sensitive and not adaptable in all applications. In [16], the PLL based on the complex filter ensures the selective sequence filtering and the attenuation of the disturbances of the distribution grid. In [17], higher harmonic attenuation and improved dynamic behavior are achieved using second- and third-order complex vectors. In the paper by Li, Weiwei, Xinbo Ruan, Chenlei Bao, Donghua Pan, and Xuehua Wang [18], a second- and third-order complex-vector-filter are proposed with the CVFM to achieve better dynamic performance or higher harmonic attenuation. Additionally, a brief comparison of each prefilter is presented. Moreover, the CVFM can be applied to the other prefilter-based grid synchronization systems. In our paper, a CVF-based control is applied to accomplish the dual functions, including harmonic filtering capability and active power injection. The proposed control has been integrated on the three-phase grid-connected PV system. The proposed control system can be effectively controlled to operate as an APF with the functionalities of source current harmonic suppression, reactive power compensation, and source current balancing. The results demonstrated in this paper clearly indicate that the presented control offers excellent performance in the case of unbalanced load. This enables the utility grid to supply the sinusoidal current. The proposed control has offered a good performance compared with PI&PLL control. Finally, it is concluded that the current is perfectly sinusoidal and does not suffer from abnormalities thanks to the CVF filter, which smoothed the load current. The load current THD is reduced from 14.64% to around 1.56% in the utility grid current. The CVF ensures robustness and stability during the synchronization between the PV and the utility grid system. The PI&PLL control presents higher active and reactive power loss pulses during synchronization. However, the CVF ensures the elimination of the reactive power fluctuations during synchronization.

In this paper, the proposed CVF-based control is developed for a three-phase grid-connected PV system. Furthermore, the harmonic-free positive sequence (HFPS) load current is used to produce referential sinusoidal currents. The salient features of this study are presented as follows:

- This control stabilizes the grid's currents under unbalanced load currents, as well as mitigates the undesirable harmonic load current while feeding the clean active power to the grid.
- The proposed control offers a high degree of immunity compared to the conventional PI&PLL controller. The AP with the proposed CVF is more robust, stable, and optimal. The key results, which are the DC offset and THD, have been significantly reduced to 1.56%.
- By adopting this controller, the voltage is improved. Moreover, the distribution grid losses are minimized, since the distance between the location of PV system and the load terminal at PCC is shorter. The harmonics in the network current are compensated according to the IEEE-519 standard, the voltage at the PCC is improved using feed-forward to minimize the switching ripple, and the current grid is balanced by avoiding oscillations under unbalanced load conditions.

The rest of paper is structured as follows: Section 2 presents components of the grid-connected PV system. Section 3 elaborates on the adopted control strategy. Section 4 presents and discusses the simulation results. Finally, the conclusions are drawn in Section 5.

2. Components of Grid-Connected Photovoltaic System

The PV system connected to the grid is shown in Figure 1. This system consists of a PV generator, a DC-DC, MPPT, DC converter link capacitor, the VSC, and LCL filter. The implementation of the proposed control strategy shows that the boost supplies the DC link with energy generated by the PV generator capacitor through adjusting the voltage of the PV generator, which coincides with the maximum power to the power curve of the PV generator.

The VSC converts the energy generated by the PV generator and supplies the power grid. The filter is used to attenuate high switching ripples and avoid resonance in the grid.

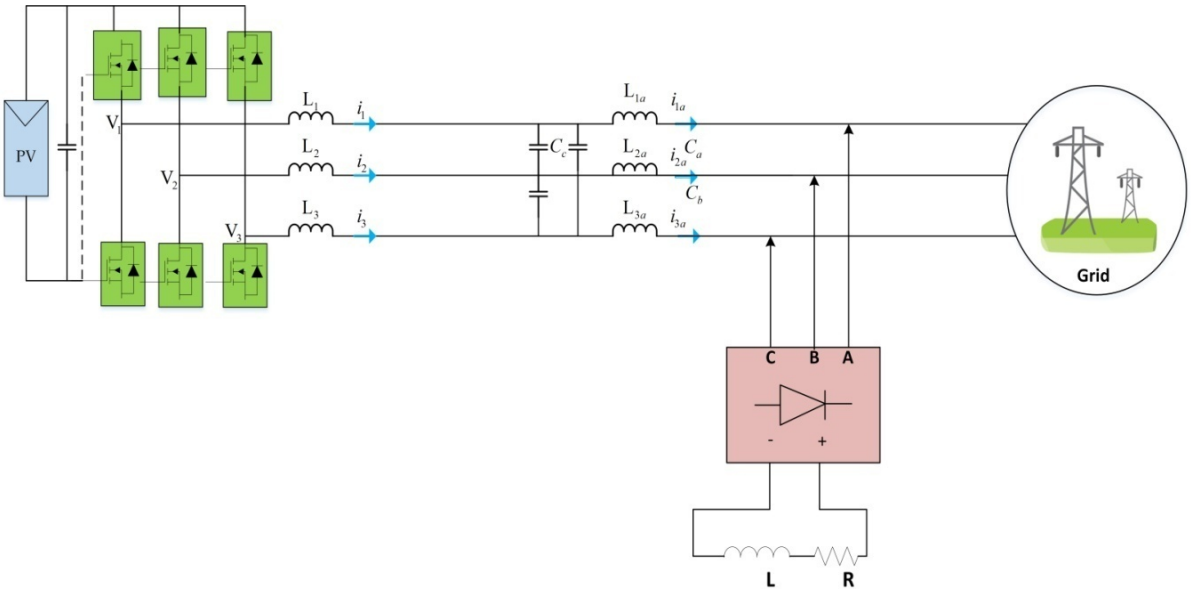

Figure 1. Main components of grid-connected PV systems.

3. Complex-Vector-Control Method

The developed control method is shown in Figure 2a,b. Both converters have their own control. Herein, the PV array voltage (Vpv) and PV array current (Ipv) are sensed, then provided to the P&O MPPT controller. The P&O MPPT controller sets the PV array set point voltage based on the estimated value that matches the maximum PV power. The PV set point voltage and the voltage on the DC link determine the duty cycle of the boost inverter. The DC-DC converter switching pulse is realized by comparing the duty cycle of the boost inverter with the high-frequency sawtooth waveform.

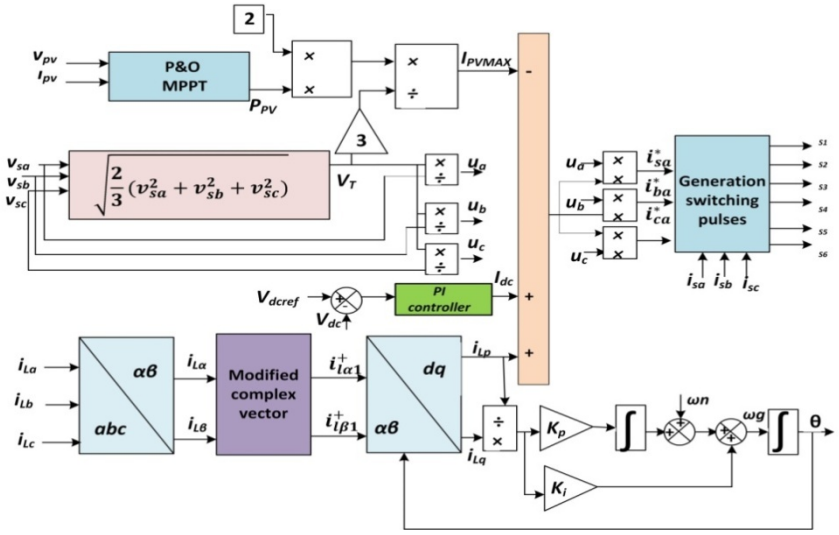

(**a**)

Figure 2. *Cont.*

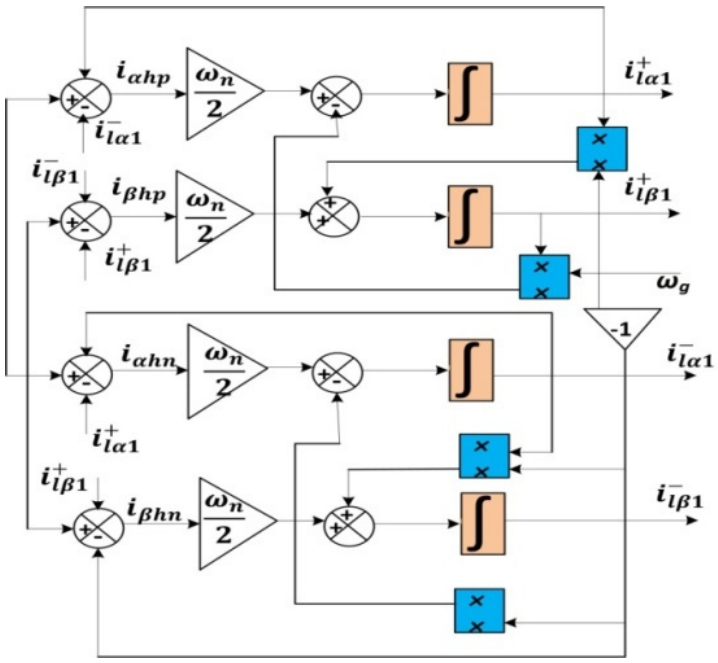

(b)

Figure 2. (**a**) Modified complex vector scheme; (**b**) modified complex-vector-filter for HFPS components extraction.

The VSC control is required to detect the distribution network current (isuv, isvw), PCC voltage (vsuv, vsvw), load current (iLuv, iLvw), and the input voltage of VSC (Vdcs). This voltage is adaptively reshaped, which refers to the voltage of the PCC, to achieve the smallest VSC switching loss. The detected grid current is compared with the reference current generated in the current controller, and the switching pulse of the VSC is performed. The VSC command is required to provide four quantities, which are identified by the AP component of the load current (ILp), the PV dynamic current (Ipvd), the DC loop voltage loss current component (ILoss), as well as the template unit used for synchronization between the grid and the PV converter.

A. Unit templates Generation

The grid line voltages V_{sab} and V_{sbc} are considered with the three-phase grid voltages V_{sa}, V_{sb}, V_{sc} extraction as follows:

$$\begin{aligned} V_{sa} &= \tfrac{1}{3}(2V_{sab} + V_{sbc}) \\ V_{sb} &= \tfrac{1}{3}(-V_{sab} + V_{sbc}) \\ V_{sc} &= \tfrac{1}{3}(-V_{sab} - 2V_{sbc}) \end{aligned} \tag{1}$$

The estimation of the PCC voltage amplitude is determined from:

$$V_{tot} = \sqrt{\frac{2}{3}(V_{sa}^2 + V_{sb}^2 + V_{sc}^2} \tag{2}$$

The three-utility grid voltage unit templates are expressed as:

$$\begin{aligned} u_1 &= \tfrac{V_{s1}}{V_{tot}} \\ u_2 &= \tfrac{V_{s2}}{V_{tot}} \\ u_3 &= \tfrac{V_{s3}}{V_{tot}} \end{aligned} \tag{3}$$

B. Evaluation of the dynamic PV current $I_{pv\max}$

The generated PV voltage and current V_{pv}, I_{pv} are herein considered, then the power of PV array is as follows:

$$P_{PV} = V_{PV} * I_{PV} \tag{4}$$

The dynamic PV current is provided by:

$$I_{PV\max} = \frac{2P_{Pv\max}}{3V_{tot}} \tag{5}$$

C. DC-Link Loss Current Evaluation

The detected VSC input voltage and the reference DC link voltage are provided to the DC voltage comparator to generate an error voltage ($V_{dcev} = V_{dcref} \times V_{dc}$), which is fed to the PI voltage controller. In this way, the continuous link loss current component (I_{dc}) is obtained.

$$I_{dc}(k) = I_{dc}(k-1) + k_p \times [V_{dcev}(k) - V_{dcev}(k-1+)] + k_i \times V_{dcev} \tag{6}$$

D. Active Power Component of Load Current Estimation

In the three-phase system, the fixed α-axis and β-axis load current components are determined from several load current phases as follows:

$$\begin{bmatrix} i_{L\alpha} \\ i_{L\beta} \end{bmatrix} = \frac{1}{\sqrt{3}} \begin{bmatrix} \frac{2}{\sqrt{3}} & -\frac{1}{\sqrt{3}} & -\frac{1}{\sqrt{3}} \\ 0 & 1 & -1 \end{bmatrix} \begin{bmatrix} i_{La} \\ i_{Lb} \\ i_{Lc} \end{bmatrix} \tag{7}$$

In-phase and quadrature harmonic-free positive sequence (HFPS) load currents and harmonic-free negative sequence (HFNS) load currents are extracted from the distorted load currents $i_{L\alpha}(k)$ and $i_{L\beta}(k)$ using the CVF. Its implementation can be obtained as follows:

The form of the typical first-order low pass scalar filter is known by the unity gain for the continuing component, mitigating the harmonics as follows:

$$L'(s) = \frac{\omega_c}{s + \omega_c} \tag{8}$$

The substitution of $s = s - j\omega_0$ into (8) results in the first complex vector, which can be written as follows:

$$L(s) = L'(s - j\omega_0) = \frac{\omega_c}{s - j\omega_0 + \omega_c} \tag{9}$$

The derivation of the CVF is implemented as follows: The SFG of (9) is shown in Figure 3b, which is transformed from Figure 3a thanks to the negative feedback.

In Figure 3b, $\frac{1}{s-j\omega_0}$ is formulated as:

$$\frac{1}{s - j\omega_0} = \frac{s + j\omega_0}{s^2 + \omega_0^2} = \frac{s}{s^2 + \omega_0^2} + j\frac{\omega_0}{s^2 + \omega_0^2} \tag{10}$$

The scalar integration of (9) is presented in Figure 3c. Figure 3d is the transformation of Figure 3c. It is known for its simplicity of the first-order CVF implementation.

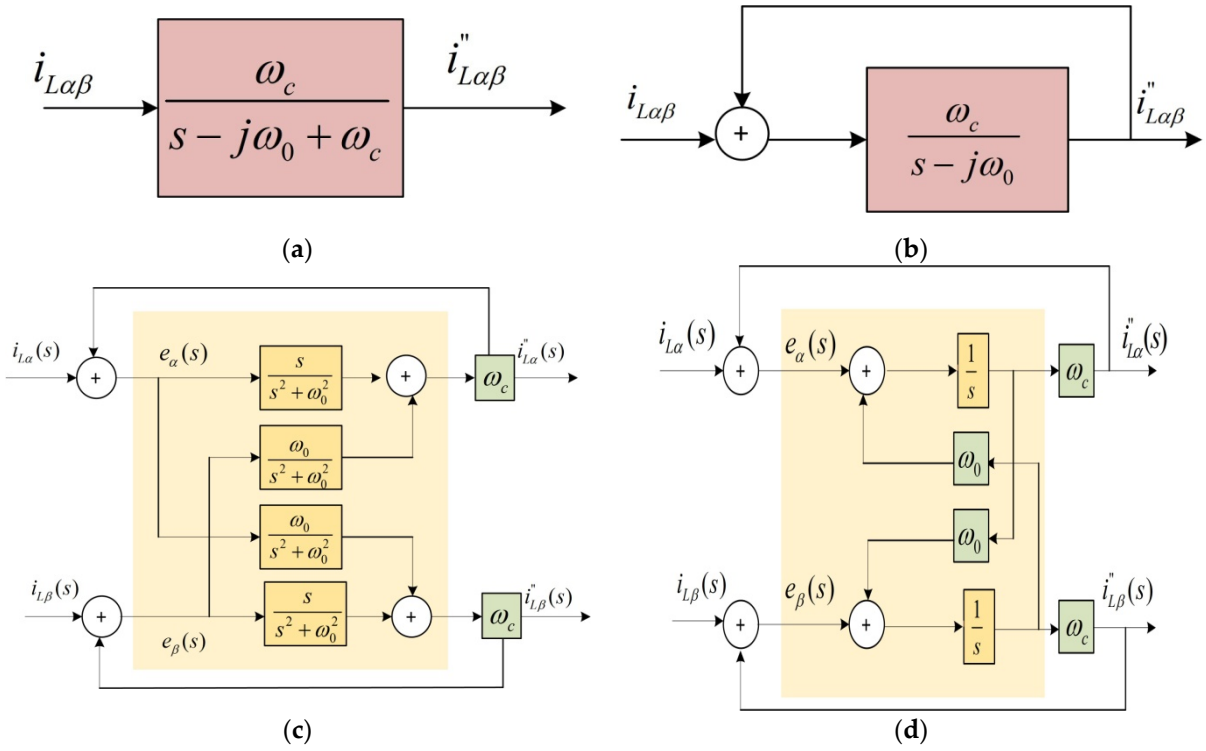

Figure 3. (**a**) Complex vector SFG; (**b**) equivalent complex vector with unity feedback structure; (**c**) scalar implementation of complex-vector-filter; (**d**) simple alternative of complex vector structure.

The value of ωc influences the dynamic response and the attenuation of the HFNS components. A higher value of ωc leads to faster dynamic response, but poor HFNS component attenuation. Therefore, to obtain a good dynamic response, and to eliminate the HFNS component, the α-axis and β-axis HFNS components are also extracted in a similar way as the HFPS components. The obtained HFNS and HFPS components are subtracted from the distorted α-axis and β-axis load currents. The ωc is chosen to be equal to 0.707 ωn to achieve a good dynamic response. Therefore, the extracted current components of HFPS and HFNS can lead to these final equations:

$$i^{+}_{L\alpha 1} = \frac{\frac{\omega_n}{\sqrt{2}}}{s - j\omega_g + \frac{\omega_n}{\sqrt{2}}}\left(i_{L\alpha}(s) - i^{+}_{L\alpha}(s) - i^{-}_{L\alpha 1}(s)\right) \tag{11}$$

$$i^{+}_{L\beta 1} = \frac{\frac{\omega_n}{\sqrt{2}}}{s - j\omega_g + \frac{\omega_n}{\sqrt{2}}}\left(i_{L\beta}(s) - i^{+}_{L\beta 1}(s) - i^{-}_{L\beta 1}(s)\right) \tag{12}$$

$$i^{-}_{L\alpha 1} = \frac{\frac{\omega_n}{\sqrt{2}}}{s + j\omega_g + \frac{\omega_n}{\sqrt{2}}}\left(i_{L\alpha}(s) - i^{+}_{L\alpha 1}(s) - i^{-}_{L\alpha 1}(s)\right) \tag{13}$$

$$i^{-}_{L\beta 1} = \frac{\frac{\omega_n}{\sqrt{2}}}{s + j\omega_g + \frac{\omega_n}{\sqrt{2}}}\left(i_{L\beta}(s) - i^{+}_{L\beta 1}(s) - i^{-}_{L\beta 1}(s)\right) \tag{14}$$

The HFPS current components $i^{+}_{L\alpha}$(s) and $i^{+}_{L\beta}$(s) are adopted to derive the active and reactive components of the load current as follows:

$$\begin{bmatrix} i_{Lp} \\ i_{Lq} \end{bmatrix} = \begin{bmatrix} \cos\omega_g t & \sin\omega_g t \\ \sin\omega_g t & \cos\omega_g t \end{bmatrix} \begin{bmatrix} i^{+}_{L\alpha} \\ i^{+}_{L\beta} \end{bmatrix} \tag{15}$$

E. Grid Frequency and Reference Angle Estimation

In the case of a large grid frequency drift, the estimated HFPS components are not orthogonal, thus the extracted AP components of the load current are not accurate. As a result, under the condition of frequency drift with minimum overshoot and settling time, it is very important to estimate the frequency of the utility grid. The accurately estimated governing equation with good dynamic response is:

$$\omega_g = \omega_n + \int k_i \left(\frac{i_{Lq}}{i_{Ld}}\right) \tag{16}$$

$$\theta = \int \left(\omega_g + k_p \frac{i_{Lq}}{i_{Ld}}\right) \tag{17}$$

F. Grid References current Estimation

The active power grid current is formulated as follows:

$$I_{pt} = I_{dc} + I_{Lp} + -I_{pv\max} \tag{18}$$

The three-phase grid reference currents are estimated, adopting the AP network current as follows:

$$\begin{aligned} i^*_{sa} &= I_{pt} \times u_a \\ i^*_{sb} &= I_{pt} \times u_b \\ i^*_{sc} &= I_{pt} \times u_c \end{aligned} \tag{19}$$

The comparison between these grid reference currents and the sensed grid currents through a comparator and feeding to a current controller can lead to the VSC control switching sequences.

4. Simulation Results

The CVF control performances have been checked through the obtained simulation results using MATLAB/SIMULINK software, and proved under different cases. The efficiency of the proposed controller is illustrated by simulation results for estimating the amplitude, phase, and dynamic response of the load current before and after filtering. The proposed control approach provides a high degree of immunity against the frequency phase shift and voltage transients in the distribution network. The simulation parameters of the implemented network support PV system are provided in Appendix A. The system model is developed for a utility grid system (UGS) via a maximum power of 80 kW and a frequency of 50 Hz. The UGS was powered by a PV system of 80 kW. The proposed CVF was evaluated in a functional grid-connected PV system.

Figures 4 and 5 present the proposed CVF performance to ensure the utility grid currents and voltages stability. The CVF ensures a proper and an optimal operation between the PV and UGS. As shown, it eliminates the fluctuations and undesirable harmonics during the simulation time.

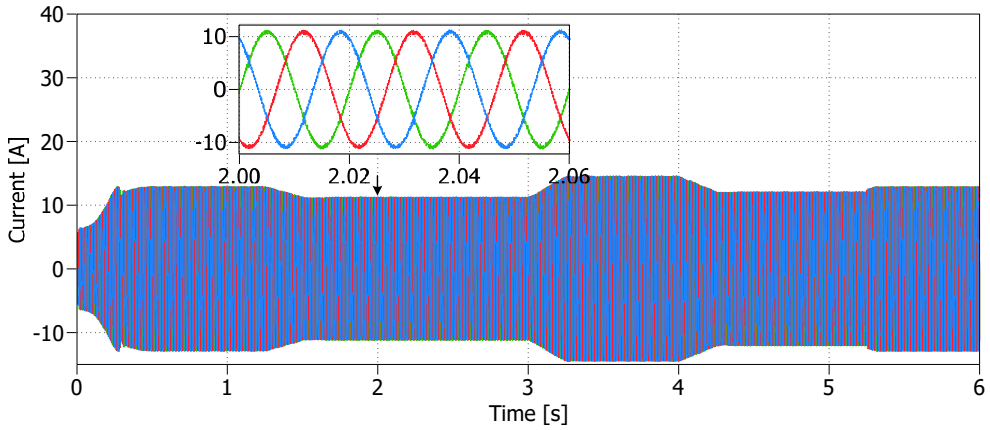

Figure 4. Grid current.

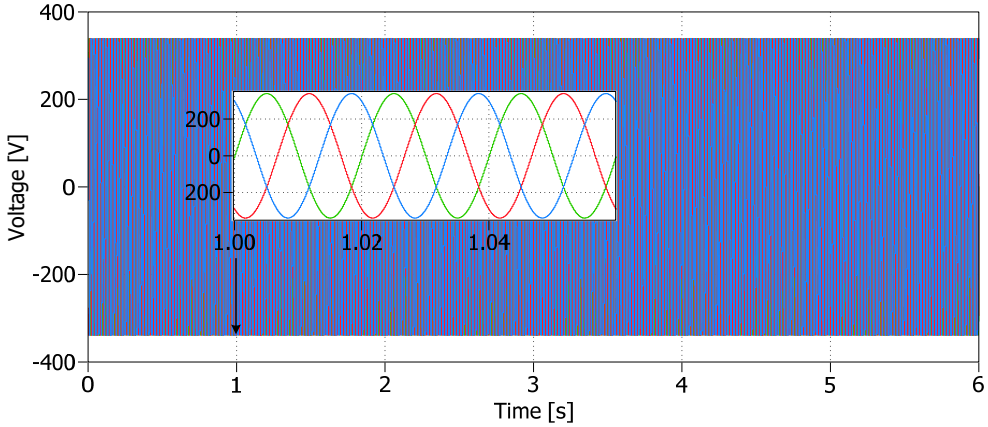

Figure 5. Grid voltage.

The proposed improved CVF method is not only used to synchronize PV converters, but contrary to PLL-based methods, it can also estimate the fundamental frequency quadrature current, which only locks the PV inverter to the network. In addition, the performance of PLL-based algorithms will significantly change with the grid voltage and frequency deviation. The fundamental frequency quadrature current components are no longer orthogonal, thus leading to the inaccurate estimation of AP component of load current. The response of the proposed control algorithm under the change in the grid angle is shown in Figure 6.

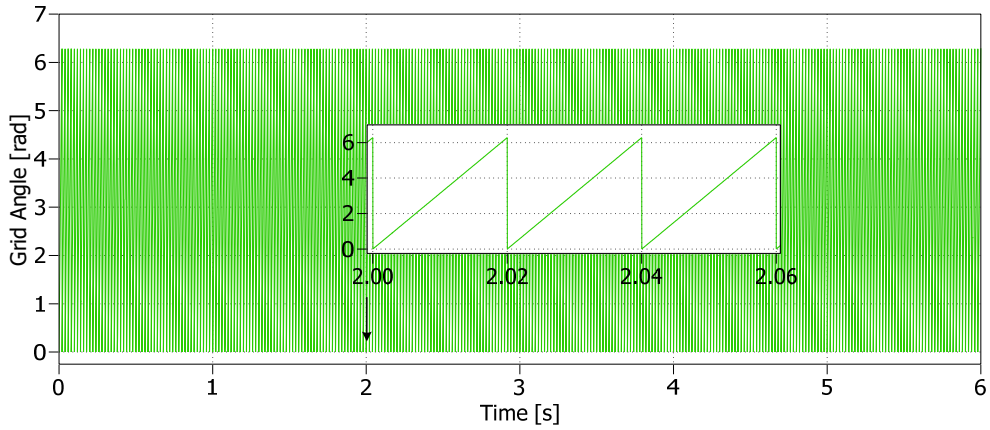

Figure 6. Grid angle variation.

The load currents comparison of various phases before and after the modified CVF is presented in Figure 7. It is observed that there is no phase shift between the input and output quantity of CVF, which illustrates that the proposed CVF provides robustness against harmonic problems.

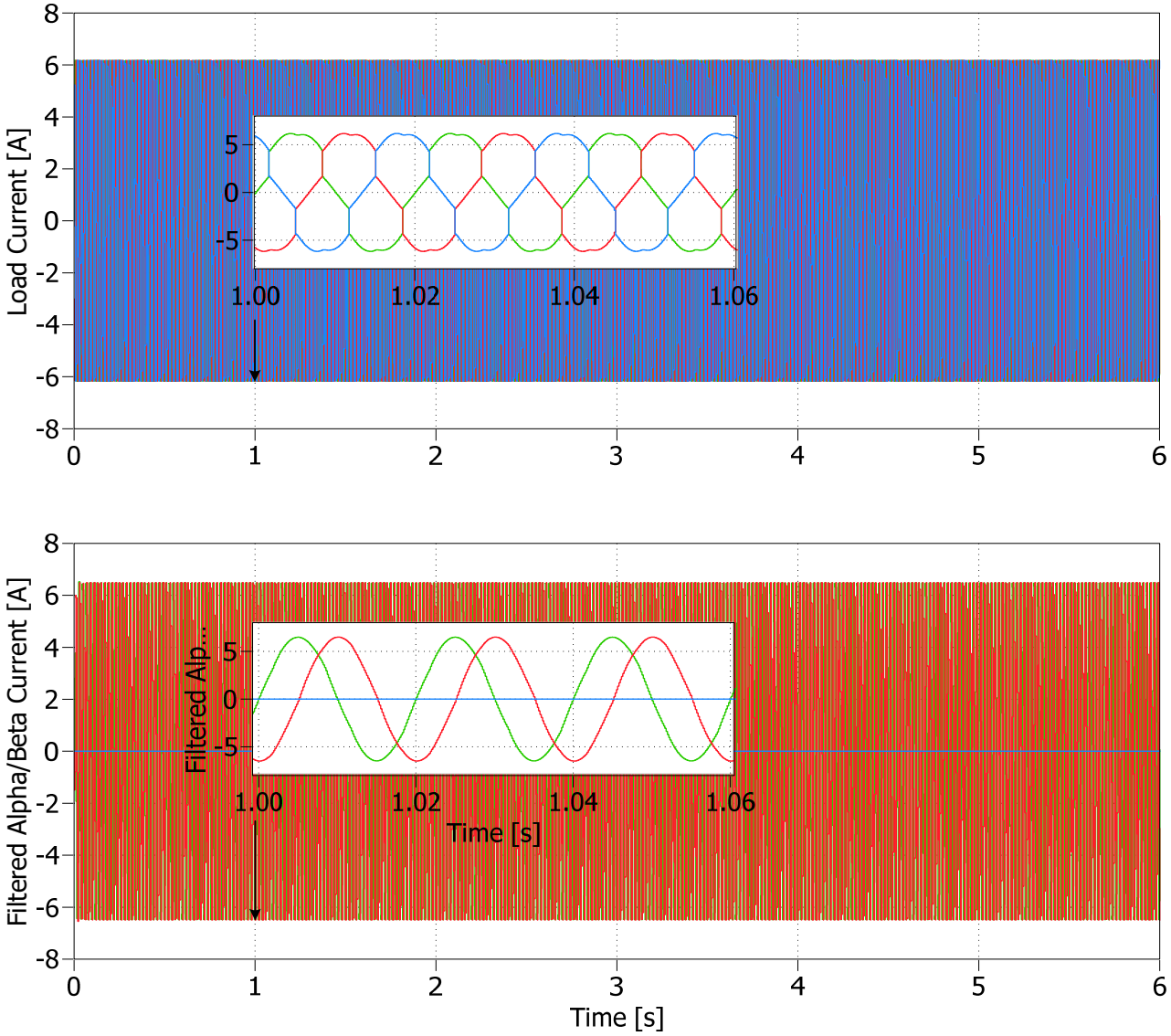

Figure 7. Load current before and after the CVF filter in alpha/beta.

It is noticeable that the current is perfectly sinusoidal and does not suffer from abnormalities thanks to the CVF filter, which smoothed the load current.

Figure 8 shows the performance of the CVF compared to the PI&PLL control. The AP with the proposed CVF is more robust, stable, and optimal compared to the PI&PLL control. From [0; 0.3] s, the CVF ensures the robustness and stability during the synchronization between the PV and UGS. The PI&PLL control presents higher active and reactive power loss pulses during synchronization. However, the CVF ensures the elimination of the RP fluctuations during synchronization (Q(VAR) = 0).

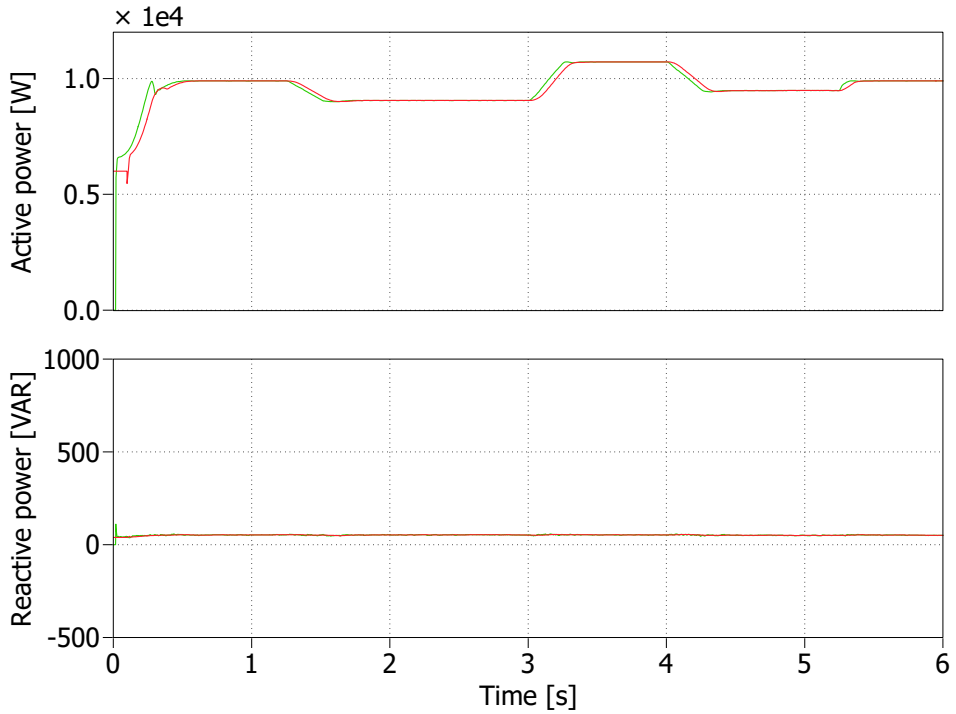

Figure 8. Active and reactive powers comparison: Red color denotes PI&PLL, while the green color denotes CVF.

At the intervals [1.5; 3.3] s and [4.3; 5.3] s, when the irradiation decreased, the PV with CVF continues to supply the maximum power to the utility grid, contrary to the PI&PLL control. Then, the CVF proves more effective, which is reasonable for use in the case of intermittent renewable sources, such as PV to decrease the irradiation conditions change impact.

Within the interval of time [3.3; 4.1] s, when using the CVF, the PV supplies only the power demand. Therefore, the CVF ensures the optimal needed power to the UGS. Compared to the PI&PLL control, which presents the reactive power fluctuation, the CVF ensures the elimination of RP fluctuations (Q(VAR) = 0).

Figure 9a,b depicts the harmonic performance before and after the CVF application. Herein, the load current THD is reduced from 14.64% to around 1.56% in the utility grid current, knowing that in [19], the total harmonic distortions value of the waveforms is 2.08%. The non-linear load value has been set according to the recommendation in the standard IEC 62040 [20]. Accordingly, the non-linear load active power is set to around 60% of the rated power of the inverter. The values of the THD in each reference cannot be clearly compared unless they are implemented on the same system and under the same conditions.

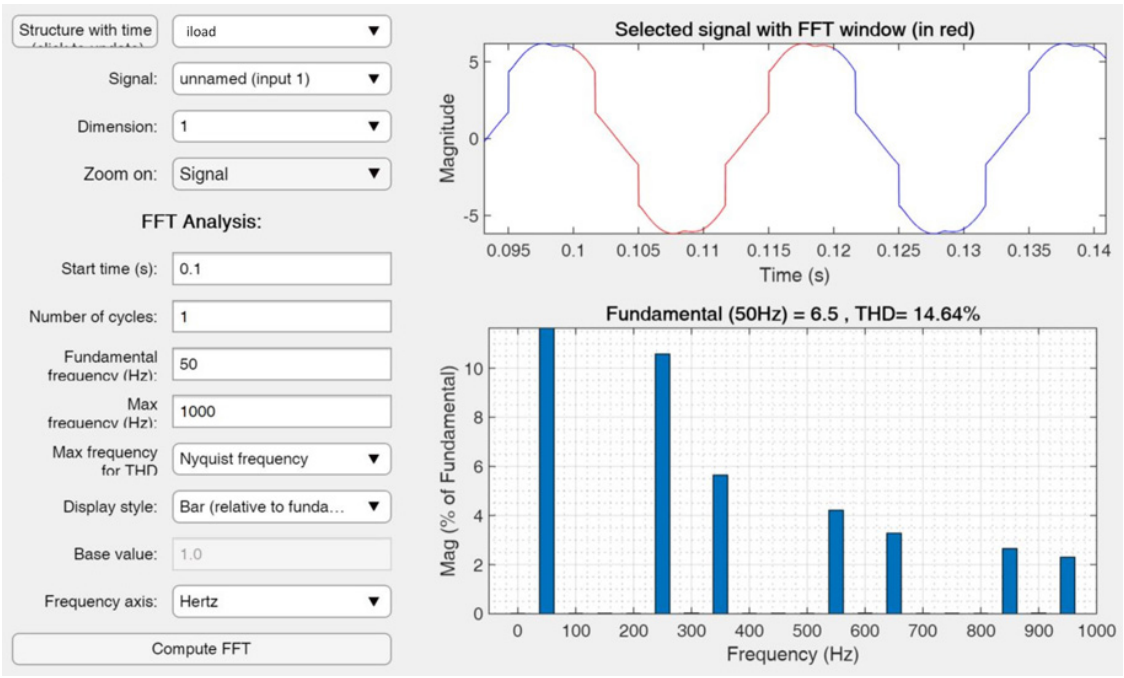

(**a**)

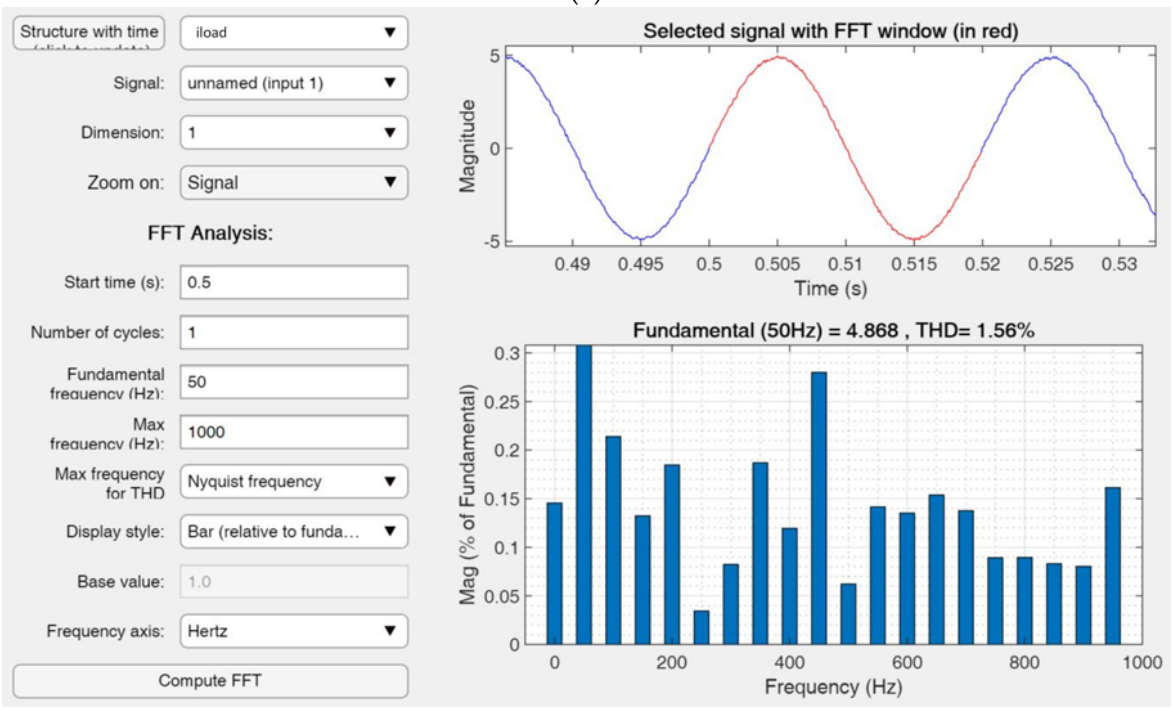

(**b**)

Figure 9. (**a**) Load current before the CVF filter; (**b**) load current after the CVF filter.

5. Conclusions

In this paper, a CVF-based control was presented to accomplish the dual functions, such as harmonic filtering capability and active power injection. The proposed control has been integrated on a three-phase grid-connected PV system. The proposed control system can be effectively controlled to operate as an APF with the functionalities of source current harmonic suppression, reactive power compensation, active power injection, and source current balancing. The results demonstrated herein clearly indicate that the presented control offers excellent performance in the case of an unbalanced load. This enables the

utility grid to supply pure sinusoidal current. The proposed control has been compared to one of the conventional solutions, where it was shown that it offers a good performance compared with PI&PLL control. Finally, the current is perfectly sinusoidal and does not suffer from abnormalities thanks to the CVF filter, which smoothed the load current. The load current THD is reduced from 14.64% to around 1.56% in the utility grid current. Furthermore, the CVF ensures robustness and stability during the synchronization between the PV and the utility grid system, while the PI&PLL control presents higher active and reactive power losses during synchronization. On the other hand, the proposed CVF ensures the elimination of the reactive power fluctuations during synchronization.

Author Contributions: Conceptualization, N.M., A.L. and J.M.G.; methodology, N.M., A.L. and S.N.; software, N.M.; validation, A.L. and N.M.; formal analysis, J.M.G. and A.C. All authors have read and agreed to the published version of the manuscript.

Funding: This work was supported by VILLUM FONDEN under the VILLUM Investigator Grant (25920): Center for Research on Microgrids.

Data Availability Statement: Not applicable.

Conflicts of Interest: The author declares no conflict of interest.

Abbreviations

AP	Active power
$i_1 i\, i_3$	Grid current
$i_{\alpha hp} i_{\beta hp} i^{+}_{L\alpha 1}$	Positive sequence harmonic currents
$i^{+}_{L\beta 1}$	HFPS current components
$i^{-}_{L\alpha 1}\ i^{-}_{L\beta 1}$	HFNS current components
RP	Reactive power
CVF	Complex-vector-filter
$C_1\, _cC_2, C_3$	Filter Capacitor
HFPS	Harmonic-free positive sequence
HFNS	Harmonic-free negative sequence
HCC	hysteretic current control (HCC)
L	Load inductance
$L_{1a}\ L_{2a}\ L_{3a}$	Grid inductance
$L_1\ L_2\ L_3$	Filter Inductance
MPPT	Maximum Power Point Tracking
PV	Photovoltaic
PI	Proportional integral
R	Load Resistance
RES	Renewable energy sources
SFG	Signal flow graph
UGS	Utility Grid System
w_f	Filter cut off frequency
w_n	Nominal frid frequency
w_g	Estimated grid frequency
VSC	Voltage source converter

Appendix A. Simulation Parameters

Ppv: 60 kW; Vdc: 789 V; grid voltage : $220\sqrt{2}$ V; nominal grid frequency: 50 Hz; LCL filter: L1 = L2: 3.6 mH/R1 = R2 = 0.04 Ω; ωn: 314 rad/s; ωc: 0.707 ωn.

References

1. Maroti, P.K.; Padmanaban, S.; Wheeler, P.; Blaabjerg, F.; Rivera, M. Modified boost with switched inductor different configurational structures for DC-DC converter for renewable application. In Proceedings of the 2017 IEEE Southern Power Electronics Conference (SPEC), Puerto Varas, Chile, 4–7 December 2017. [CrossRef]
2. D'Adamo, I.; Gastaldi, M.; Morone, P. The post COVID-19 green recovery in practice: Assessing the profitability of a policy proposal on residential photovoltaic plants. *Energy Policy* **2020**, *147*, 111910. [CrossRef] [PubMed]

3. Abidin, M.Z.; Mahyuddin, M.; Zainuri, M.M. Solar Photovoltaic Architecture and Agronomic Management in Agrivoltaic System: A Review. *Sustainability* **2021**, *13*, 7846. [CrossRef]
4. Mansouri, N.; Lashab, A.; Sera, D.; Guerrero, J.M.; Cherif, A. Large Photovoltaic Power Plants Integration: A Review of Challenges and Solutions. *Energies* **2019**, *12*, 3798. [CrossRef]
5. Mansouri, N.; Lashab, A.; Guerrero, J.M.; Cherif, A. Photovoltaic power plants in electrical distribution networks: A review on their impact and solutions. *IET Renew. Power Gener.* **2020**, *14*, 2114–2125. [CrossRef]
6. Ardashir, J.F.; Sabahi, M.; Hosseini, S.H.; Blaabjerg, F.; Babaei, E.; Gharehpetian, G.B. Transformerless Inverter with Charge Pump Circuit Concept for PV Application. *IEEE J. Emerg. Sel. Top. Power Electron.* **2016**. Accepted. [CrossRef]
7. Xiao, W.; El Moursi, M.; Khan, O.; Infield, D. Review of grid-tied converter topologies used in photovoltaic systems. *IET Renew. Power Gener.* **2016**, *10*, 1543–1551. [CrossRef]
8. Hanif, M.; Khadkikar, V.; Xiao, W.; Kirtley, J.L. Two Degrees of Freedom Active Damping Technique for LCL Filter-Based Grid Connected PV Systems. *IEEE Trans. Ind. Electron.* **2013**, *61*, 2795–2803. [CrossRef]
9. Azani, H.; Massoud, A.; Benbrahim, L.; Williams, B.W.; Holiday, D. An LCL filter-based grid-interfaced three-phase voltage source inverter: Performance evaluation and stability anaylsis. In Proceedings of the 7th IET International Conference on Power Electronics, Machines and Drives (PEMD), Manchester, UK, 8–10 April 2014.
10. Zeng, Z.; Yang, H.; Zhao, R.; Cheng, C. Topologies and control strategies of multi-functional grid-connected inverters for power quality enhancement: A comprehensive review. *Renew. Sustain. Energy Rev.* **2013**, *24*, 223–270. [CrossRef]
11. Jin, L.; Haosong, L.; Zhongping, X.; Ting, W.; Shuai, W.; Yutong, W.; Dongliang, H.; Chunting, K.; Jia, W.; Dan, S. Research on Wide-area Distributed Power Quality Data Fusion Technology of Power Grid. In Proceedings of the 2019 IEEE 4th International Conference on Cloud Computing and Big Data Analysis (ICCCBDA), Chengdu, China, 12–15 April 2019; pp. 185–188. [CrossRef]
12. Singh, B.; Chandra, A.; Al-Haddad, K. Power Quality Problems and Mitigation Techniques. In *Power Quality Problems and Mitigation Techniques BOOK*; John Wiley and Sons Ltd.: Hoboken, NJ, USA, 2015. [CrossRef]
13. Hannan, M.A.; Ghani, Z.A.; Mohamed, A.; Uddin, M.N. Real-Time Testing of a Fuzzy-Logic-Controller-Based Grid-Connected Photovoltaic Inverter System. *IEEE Trans. Ind. Appl.* **2015**, *51*, 4775–4784. [CrossRef]
14. Soreng, B.; Garnayak, R.; Pradhan, R. A Synchronous Reference Frame based PLL Control for a Grid-Tied Photovoltaic System. In Proceedings of the 2017 International Conference on Current Trends in Computer, Electrical, Electronics and Communication (CTCEEC), Mysore, India, 8–9 September 2017; pp. 1017–1022. [CrossRef]
15. Yazdani, D.; Bakhshai, A.; Joos, G.; Mojiri, M. A Real-Time Extraction of Harmonic and Reactive Current in a Nonlinear Load for Grid-Connected Converters. *IEEE Trans. Ind. Electron.* **2009**, *56*, 2185–2189. [CrossRef]
16. Ramezani, M.; Golestan, S.; Li, S.; Guerrero, J.M. A simple approach to enhance the performance of Complex-coefficient filter-based PLL in grid-connected applications. *IEEE Trans. Ind. Electron.* **2018**, *65*, 5081–5085. [CrossRef]
17. Yuan, X.; Allmeling, J.; Merk, W.; Stemmler, H. Stationary frame generalized integrators for current control of active power filters with zero steady state error for current harmonics of concern under unbalanced and distorted operation conditions. *IEEE Trans. Ind. Appl.* **2002**, *32*, 523–532. [CrossRef]
18. Li, W.; Ruan, X.; Bao, C.; Pan, D.; Wang, X. Grid Synchronization Systems of Three-Phase Grid-Connected Power Converters: A Complex-Vector-Filter Perspective. *IEEE Trans. Ind. Electron.* **2013**, *61*, 1855–1870. [CrossRef]
19. Patel, N.; Kumar, A.; Gupta, N. Three-Phase Single-Stage VSC Controlled Solar Photovoltaic System with Harmonic Filtering Capability Applied to DG. In Proceedings of the 2019 IEEE 2nd International Conference on Power and Energy Applications (ICPEA), Singapore, 27–30 April 2019. [CrossRef]
20. IEC. IEC 62040-1:2017+AMD1:2021 CSV | IEC Webstore. [Online]. Available online: https://webstore.iec.ch/publication/69012 (accessed on 12 February 2022).